Materials Advances

Accepted Manuscript

This article can be cited before page numbers have been issued, to do this please use: L. Loghina, J. Jancalek, Z. Zmrhalova, R. Jambor, Z. Ruzickova, A. Imramovský, S. Podzimek and M. Vlcek, *Mater. Adv.*, 2026, DOI: 10.1039/D6MA00406G.

ROYAL SOCIETY OF CHEMISTRY

rsc.li/materials-advances

View Article Online
DOI: 10.1039/D6MA00406G

ARTICLE

Design and synthesis of thiophene-engineered phenanthroimidazoles with vinyl functionality for polymer integration

Received 00th January 20xx,
Accepted 00th January 20xx

DOI: 10.1039/x0xx00000x

Liudmila Loghina*[a], Jiri Jancalek[a], Zuzana Zmrhalova[a], Roman Jambor[b], Zdena Ruzickova[b], Ales Imramovsky[c], Stepan Podzimek[d,e] and Miroslav Vlcek[a,b]

We report the first systematic design of thiophene-engineered phenanthro[9,10-*d*]imidazoles (PPIs) that combine C2 sulfur-containing π-aryl substitution with N1 styryl functionality, enabling direct polymer integration. Thiophene, benzo[*b*]thiophene, and thieno[3,2-*b*]thiophene fragments were introduced at the C2 position to control the electronic structure of the phenanthroimidazole chromophore, while a vinyl group at the N1-aryl fragment provides a polymerizable handle for incorporation as comonomers during radical copolymerization. The target compounds were synthesized via a modular strategy based on Debus-Radziszewski condensation, followed by Suzuki-Miyaura cross-coupling and were comprehensively characterized by spectroscopic, structural, and thermal methods. Density functional theory (DFT) calculations were performed to elucidate the frontier molecular orbital distribution and support the experimentally observed optical properties. Photophysical investigations reveal that C2 sulfur-containing substitution provides an efficient handle for tuning emission properties, leading to gradual bathochromic shifts and controlled modulation of the optical band gap while preserving structured blue to blue-green fluorescence with photoluminescence quantum yields reaching up to 86%. In contrast, the N1 styryl functionality remains electronically decoupled from the emissive core, allowing polymerization without significantly perturbing the intrinsic optical properties of the chromophore. Radical copolymerization with N-vinylcarbazole affords luminescent polymeric materials retaining the characteristic emission behavior of the corresponding monomers. Overall, this work establishes a molecular design strategy in which electronic tuning of the phenanthroimidazole chromophore and polymer processability are effectively decoupled within a single scaffold, providing access to processable luminescent materials with predictable and tunable optical properties.

Introduction

1-Phenyl-phenanthro[9,10-*d*]imidazoles (PPI) represent an important class of rigid, polyaromatic heterocycles that have attracted increasing attention as deep-blue and blue-green emitters in optoelectronic applications.[1-5] Their highly planar π-conjugated cores support structured emission with characteristic vibronic progression, while their synthesis is straightforward, typically involving a one-pot Debus-Radziszewski condensation.[6,7] Structural modification of PPIs offers a convenient route to tune absorption and emission properties, improve photoluminescence quantum yields (PLQYs), and control aggregation behaviour. Most studies to date have focused on variation of the N1-aryl fragment, including phenyl, biphenyl, and vinyl-aryl substituents, to modulate the optical gap and solid-state packing.[8-10]

Sulfur-containing aromatic fragments, particularly thiophene, benzo[*b*]thiophene, and thieno[3,2-*b*]thiophene, are widely employed as electron-rich, π-conjugated building blocks in organic semiconductors and emissive materials due to their ability to enhance delocalization, improve planarity, and strengthen intermolecular interactions such as π-π stacking.[11-13] These S-aryl units are common in D-π-A-π-D architectures, for example, in thiophene/benzothiadiazole tandems designed to boost aggregation-induced emission (AIE) or induce bathochromic shifts.[14] Despite their proven utility in other π-conjugated systems, S-aryl substituents have rarely been introduced deliberately at the C2 position of 1-phenyl-phenanthro[9,10-*d*]imidazoles (PPIs), and their influence on the spectral properties and processability of these compounds has not yet been systematically investigated. Thiophene-containing phenanthro[9,10-*d*]imidazoles have previously been reported as functional luminescent materials, where thienyl-type substituents were shown to influence thermal, electrochemical, and optical properties of the phenanthroimidazole core.[15] These studies demonstrate the potential of sulfur-containing aromatic fragments for tuning molecular properties within this

[a] Center of Materials and Nanotechnologies, Faculty of Chemical Technology, University of Pardubice, 530 02 Pardubice, Czech Republic.
[b] Department of General and Inorganic Chemistry, Faculty of Chemical Technology, University of Pardubice, 532 10 Pardubice, Czech Republic.
[c] Institute of Organic Chemistry and Technology, Faculty of Chemical Technology, University of Pardubice, 53210 Pardubice, Czech Republic.
[d] Department of Chemistry and Technology of Macromolecular Materials, Faculty of Chemical Technology, University of Pardubice, 532 10 Pardubice, Czech Republic.
[e] Synpo, a. s., S. K. Neumanna 1316, 532 07 Pardubice, Czech Republic.
* Correspondence: Liudmila.Loghina@upce.cz.

class of compounds. The novelty of the present study does not lie solely in the use of thiophene-derived substituents, but in the first systematic combination of C2 sulfur-containing π-aryl tuning with an N1 styryl polymerizable handle within one phenanthroimidazole scaffold. This design enables direct comparison between molecular and polymer-bound states while preserving the intrinsic emissive characteristics of the chromophore.

In contrast, structural modification at the N1-aryl position of PPIs has been more extensively investigated, with reported examples predominantly featuring simple phenyl or biphenyl substituents to tune the optical gap and influence solid-state packing.[16] Only a limited number of studies have addressed extended π-aryl substitution at the N1 position of PPI, and vinyl-aryl derivatives remain largely unexplored, with only very recent examples reported. Our recent work presented the first synthesis and photophysical characterization of N1-vinyl-biphenyl PPIs, highlighting their potential as reactive handles for post-functionalization and incorporation into polymer matrices.[17] Beyond spectral tuning, polymerization strategies to obtain processable emissive materials include embedding PPI dyes into polymer backbones, for example, by tethering phenanthroimidazole chromophores to a polynorbornene scaffold via ROMP, which stabilizes the chromophore environment and prevents phase separation.[18] More broadly, the field has shown that incorporating polymerizable moieties (e.g., vinyl, (meth)acrylate, styryl handles) on luminogens enables direct participation in radical/controlled polymerizations, improving film integrity and suppressing dopant migration; this concept is well established for AIE/luminogenic systems and polymer networks.[19,20] However, to the best of our knowledge, PPI structures featuring C2-S-aryl substitution have not been reported, and N1-styryl derivatives are likewise absent from the literature. The present work is the first to merge these two design elements within a single molecular scaffold, enabling simultaneous modulation of photophysical properties and the introduction of polymerizable functionality.

In this work, phenanthro[9,10-*d*]imidazole derivatives were designed to combine targeted electronic modulation with polymer compatibility within a single molecular scaffold. The electronic structure of the emissive core was tuned through substitution at the C2 position using sulfur-containing aromatic fragments - thiophene (Th), benzo[*b*]thiophene (BTh), and thieno[3,2-*b*]thiophene (TTh), which were selected to provide a controlled increase in conjugation and rigidity while maintaining a comparable molecular framework. In parallel, a styryl group was introduced at the N1-aryl position to serve as a polymerizable handle, enabling incorporation as comonomers during radical copolymerization. This dual design allows independent control over photophysical tuning and processability: the C2 substituent governs the optical response of the phenanthroimidazole chromophore, while the N1 styryl functionality enables polymer integration without extending the conjugation of the emissive core. This approach provides an initial proof-of-concept for the incorporation of the developed emissive monomers into polymeric materials. Such functional decoupling enables systematic structure-property studies in both molecular and polymer-bound states without significantly perturbing the intrinsic electronic structure of the phenanthroimidazole core.

Experimental

General procedure for the synthesis of halogenated phenanthroimidazoles (Debus-Radziszewski condensation)

A mixture of phenanthrene-9,10-dione (0.01 mol), the corresponding aniline (4-iodo- or 4-bromoaniline, 0.03 mol), and ammonium acetate (0.02 mol) was suspended in glacial acetic acid (50 ml) under an argon atmosphere. While stirring, the corresponding aldehyde (0.01 mol) was added, and the reaction mixture was stirred for 10 min at room temperature, then refluxed for 4-6 hours until complete conversion (monitored by TLC in CH_2Cl_2). After cooling to room temperature, the mixture was diluted with an equal volume of water. The precipitated solid was filtered, washed with water and ethanol, and air-dried. The crude product was purified by column chromatography on silica gel using dichloromethane as the eluent.

General procedure for the Suzuki-Miyaura cross-coupling

A halogenated phenanthroimidazole (0.005 mol) was placed in a round-bottom flask along with toluene (60 ml) and ethanol (20 ml). A solution of potassium carbonate (0.015 mol) in water (7.5 ml) was added, and several argon purges degassed the resulting biphasic mixture. Then, (4-vinylphenyl)boronic acid (0.0055 mol) and tetrakis(triphenylphosphine)palladium(0) (0.29 g) were added under argon. The reaction mixture was degassed again and refluxed for 5-8 h until complete conversion (monitored by TLC). After cooling, the mixture was diluted twofold with ethanol, and the precipitated solid was collected by filtration, washed thoroughly with water and ethanol, and air-dried. The crude product was purified by column chromatography on silica gel using dichloromethane as the eluent.

Radical Copolymerization

Radical copolymerization of the three phenanthroimidazole-based vinyl monomers (5 wt.%) was performed under identical conditions. This composition corresponds to a low molar fraction of the emissive monomerwithin the polymeric material and minimizing aggregation effects. Each monomer (0.10 g, 5 wt.%) was reacted with N-vinylcarbazole (2.0 g, 10.6 mmol) in dry 1,2-dichlorobenzene (12 ml) using azobisisobutyronitrile (AIBN, 0.03 g, 0.18 mmol) as a radical initiator. The mixture was degassed, backfilled with argon, sealed, and stirred at 75 °C for 48 hours. After cooling to room temperature, the reaction mixture was poured into hexane (100 ml). The resulting precipitate was filtered, thoroughly washed with hexane, and dried under vacuum. The copolymers obtained appeared as off-white powders: P(Th-VPPI-co-VK): yield 1.9 g; P(BTh-VPPI-co-VK): yield 2.0 g; P(TTh-VPPI-co-VK): yield 1.8 g.

Crystallography

Single crystals of BTh-PPI-I, TTh-PPI-Br and TTh-VPPI were obtained from CH_2Cl_2/petroleum ether (5:1) by slow

View Article Online
DOI: 10.1039/D6MA00486C

evaporation at room temperature. Diffraction data for BTh-PPI-I, TTh-PPI-Br and TTh-VPPI were collected using a Bruker Venture D8 diffractometer at 150 K with graphite-monochromated Mo-Ka (0.7107 Å) radiation. The frames were integrated into the Bruker SAINT software package using a narrow-frame algorithm. Data were corrected for absorption effects using the Multi-Scan method (SADABS). The obtained data were treated by the XT-version 2014/5 and SHELXL-2019/1 software implemented in APEX4 v2021.10-0 (Bruker AXS) system. All non-hydrogen atoms were refined using anisotropic displacement parameters. Crystallographic data for the structural analyses have been deposited with the Cambridge Crystallographic Data Centre, CCDC nos. 2528847-2528849. Copies of this information may be obtained free of charge from The Director, CCDC, 12 Union Road, Cambridge CB2 1EY, UK (fax: +44-1223-336033; e-mail: deposit@ccdc.cam.ac.uk or www: http://www.ccdc.cam.ac.uk).

Results and discussion

Molecular design, synthesis, and structural features.

The molecular design of the present series was guided by two complementary objectives: (i) systematic modulation of the electronic structure of 1-phenyl-phenanthro[9,10-*d*]imidazoles through C2 substitution with sulfur-containing π-conjugated fragments, and (ii) introduction of a polymerizable handle at the N1-aryl position to enable incorporation as comonomers during radical copolymerization. Phenanthroimidazole was selected as a rigid, polycyclic acceptor-emitter core due to its high thermal stability, pronounced vibronic emission, and well-established synthetic accessibility. To probe the influence of sulfur-rich aromatic substituents, three thiophene-derived units with gradually increasing π-extension and rigidity were introduced at the C2 position: thiophene (Th), benzo[*b*]thiophene (BTh), and thieno[3,2-*b*]thiophene (TTh). This series enables a controlled comparison of conjugation length, sulfur content, and molecular planarity while preserving the same phenanthroimidazole backbone. From a molecular design perspective, these fragments represent a progression from a relatively flexible five-membered heteroaromatic ring (Th) to fused bicyclic sulfur-containing systems, namely BTh and TTh, which differ in heteroatom density and conjugation topology rather than in ring count.

The synthesis of the halogenated phenanthroimidazole precursors (Th-PPI-I, BTh-PPI-I, and TTh-PPI-Br) was accomplished via a classical Debus-Radziszewski condensation of phenanthrene-9,10-dione with the corresponding aldehydes and p-halogenated anilines (Scheme 1). This one-pot protocol afforded the target compounds in high yields (79-89%) and was tolerant of heteroaromatic sulfur-containing aldehydes. Importantly, the use of p-iodo- or p-bromophenyl substituents at the N1 position provided a versatile reactive site for subsequent cross-coupling without perturbing the phenanthroimidazole core.

Structural integrity and purity of the halogenated intermediates were confirmed by multinuclear NMR spectroscopy, FTIR spectroscopy, elemental analysis, and, for selected compounds, single-crystal X-ray diffraction (see *ESI*). The NMR spectra consistently displayed the characteristic downfield-shifted imidazole and phenanthrene protons, while signals attributable to the thiophene-based substituents confirmed their successful incorporation. FTIR spectra showed diagnostic C=N stretching vibrations of the imidazole ring (~1610 cm^{-1}) together with distinct C-S vibrational modes whose position depended on the nature of the sulfur-containing fragment. The vinyl-functionalized target monomers (Th-VPPI, BTh-VPPI, and TTh-VPPI) were obtained by Suzuki-Miyaura cross-coupling of the halogenated precursors with (4-vinylphenyl)boronic acid.

View Article Online
DOI: 10.1039/D6MA00406G

ARTICLE

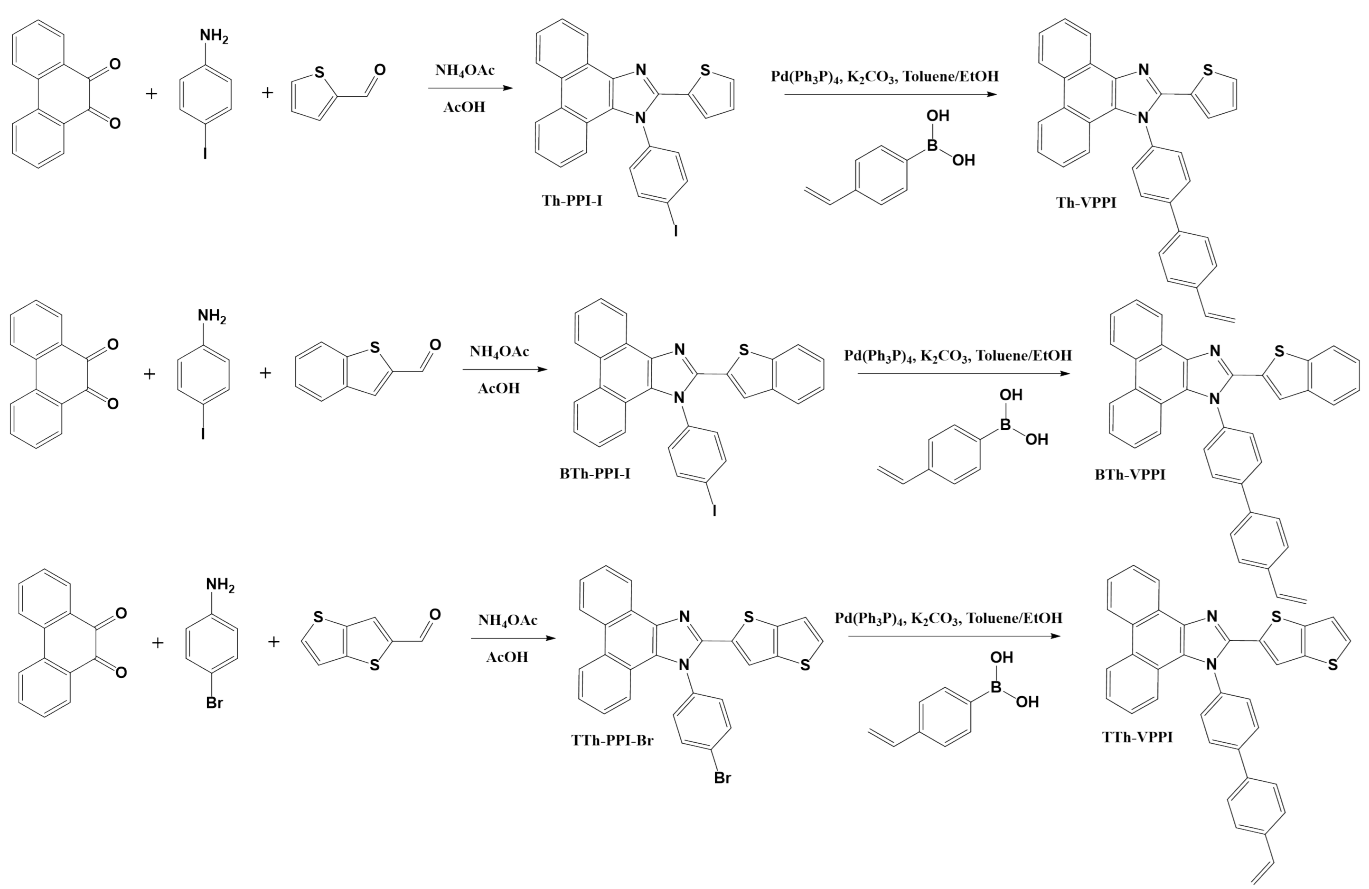

Scheme 1. Synthetic routes to thiophene-engineered phenanthro[9,10-*d*]imidazoles and their vinyl-functionalized derivatives used for polymer integration.

This transformation proceeded smoothly under mild biphasic conditions and afforded the desired styryl-type derivatives in good yields (76-81%). Introduction of the vinyl group was unambiguously confirmed by the appearance of characteristic vinyl proton resonances in the ^{1}H NMR spectra (δ ≈ 5.3-5.9 and 6.7-6.8 ppm) and by the emergence of a C=C stretching band near 985-990 cm^{-1} in the FTIR spectra. Notably, the phenanthroimidazole core and the C2-thiophene-derived substituents remained spectroscopically unchanged during the coupling reaction, indicating that the cross-coupling selectively functionalized the N1-aryl moiety. In addition to the characteristic downfield-shifted resonances of the phenanthroimidazole core, the ^{1}H NMR spectra revealed well-resolved signals attributable to the thiophene-based substituents at the C2 position. For Th-containing derivatives, the thiophene protons appeared as characteristic doublets and multiplets in the 6.8-7.1 ppm region, consistent with a monosubstituted thiophene ring. In the case of benzo[*b*]thiophene and thieno[3,2-*b*]thiophene substituents, the aromatic proton patterns were shifted further downfield (≈7.0-7.6 ppm). They exhibited increased signal dispersion, reflecting higher annulation and more rigid fused-ring structures. These features provide clear spectroscopic confirmation of the successful incorporation of the respective sulfur-containing fragments.

^{1}H NMR spectra of the copolymers were recorded; however, due to the low content of the phenanthroimidazole units (approximately 2 mol%) and significant overlap of signals with the poly(N-vinylcarbazole) backbone in the aromatic region, quantitative determination of the comonomer ratio was not feasible. This limitation is consistent with previously reported PVK-based systems.[21]

Compounds BTh-PPI-I, TTh-PPI-Br and TTh-VPPI were unambiguously characterized by single-crystal X-ray diffraction analysis. Single crystals of BTh-PPI-I and TTh-PPI-Br were obtained from CH_2Cl_2/petroleum ether (5:1), and molecular structures are depicted in Figure 1, together with selected

View Article Online
DOI: 10.1039/D5MA00486G

bonds and angles (for selected crystallographic parameters, see Table S1).

The halogenated phenanthroimidazole precursors BTh-PPI-I and TTh-PPI-Br contain central phenanthroimidazole substituted by benzo[*b*]thiophene (BTh), and thieno[3,2-*b*]thiophene (TTh) at the C1 atom. Both sulfur-containing heteroaromates are coupled by C1-C22 bonds with 1.451(2) Å and 1.454(4) Å bond lengths, defining the presence of a C-C covalent bond ($S_{cov}C,C$ = 1.5 Å). The p-iodo- and p-bromophenyl substituents are coupled at the N1 atom of phenanthroimidazole by N1-C16 bonds with 1.435(2) Å and 1.437(2) Å bond lengths, respectively, defining the presence of N-C single bond ($S_{cov}C,N$ = 1.46 Å).[22]

Single crystals of vinyl-functionalized TTh-VPPI, obtained by Suzuki-Miyaura cross-coupling of the halogenated precursor TTh-PPI-Br with (4-vinylphenyl)boronic acid, were obtained from CH_2Cl_2/petroleum ether (5:1). The molecular structure is depicted in Figure 2 together with selected bonds and angles (for selected crystallographic parameters see Table S1). The molecule of TTh-VPPI contains a central phenanthroimidazole substituted by thieno[3,2-*b*]thiophene (TTh) at the C2 atom. The C1-C22 bond length 1.456(2) Å is similar to that of the TTh-PPI-Br precursor and defines a single C-C covalent bond ($S_{cov}C,C$ = 1.5 Å). The 4-vinylphenyl group is coupled to the original p-bromophenyl group by a new C25-C28 bond. The C25-C28 bond length (1.484(3) Å) suggests the presence of a new C-C single bond and forms a 4-vinyl-biphenyl substituent that is coupled at the N1 atom of phenanthroimidazole by N1-C16 bond with 1.437(3) Å bond length, defining the presence of an N-C single bond ($S_{cov}C,N$ = 1.46 Å).[22] In contrast, the C34-C35 bond length (1.323(4) Å) clearly defined the presence of a C-C double bond in the 4-vinyl-biphenyl substituent.

Figure 1. ORTEPs of BTh-PPI-I and TTh-PPI-Br. 50% probability ellipsoids represent non-H atoms. H atoms are omitted for clarity. For BTh-PPI-I: Bond lengths (Å): I1-C19 2.100(2); S1-C22 1.748(2); S1-C23 1.739(2); N1-C1 1.380(2); N1-C2 1.389(2); N1-C16 1.435(2); C1-C22 1.451(2). For TTh-PPI-Br: Bond lengths (Å): Br1-C25 1.894(2); S1-C22 1.748(2); S1-C23 1.719(2); N1-C1 1.379(3), N1-C2 1.398(3); N1-C16 1.437(2); C1-C22 1.454(4).

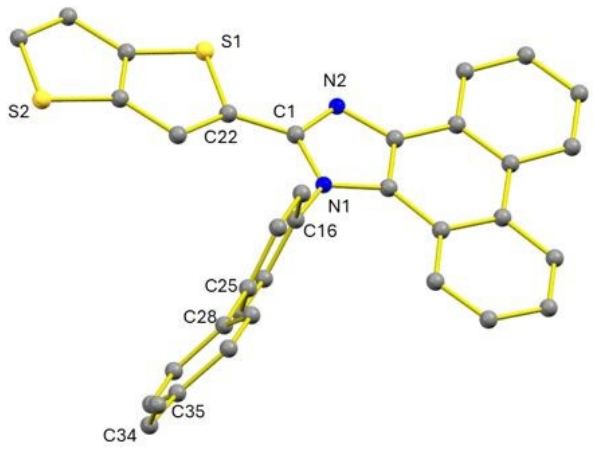

Figure 2. ORTEPs of TTh-VPPI. 50% probability ellipsoids represent non-H atoms. H atoms are omitted for clarity. Bond lengths (Å): S1-C22 1.741(2); S1-C23 1.716(2); N1-C1 1.378(2); N1-C2 1.394(2); N1-C16 1.437(3); C1-C22 1.456(2); C25-C28 1.484(3); C34-C35 1.323(4).

From a structural standpoint, the resulting VPPI monomers combine a rigid, planar phenanthroimidazole-thiophene chromophore with a peripheral styryl group spatially separated from the emissive core. This architectural feature is essential for preserving the chromophore's intrinsic photophysical properties while enabling radical copolymerization. The vinyl group does not extend the conjugation of the phenanthroimidazole core directly but instead serves as a chemically orthogonal functionality for polymer integration. Overall, this synthetic strategy provides a modular and versatile platform for preparing thiophene-engineered phenanthroimidazoles with tunable electronic structures and built-in processability. The combination of C2 sulfur-containing π-systems with N1-styryl functionality represents a previously unexplored design space for phenanthroimidazole-based luminogens and sets the stage for systematic investigation of structure-property relationships in both molecular and polymer-bound forms. The combination of crystallographic analysis and theoretical calculations provides direct insight into how subtle structural variations influence the electronic structure of the chromophores.

Structural and thermal characterization of monomers and copolymers

View Article Online
DOI: 10.1039/D6MA00406G

FTIR spectra of the copolymers were almost identical to that of pure poly(N-vinylcarbazole), reflecting the dominant contribution of the polymer matrix at a 5 wt.% (≈2 mol%) chromophore loading and the overlap of aromatic vibrational bands, which contributes to the phenanthroimidazole units being indistinguishable in the spectra (Fig. S34, ESI). Nevertheless, the characteristic vinyl absorptions of N-vinylcarbazole at 1640, 1367, 1295 and 961 cm^{-1} were completely absent in all spectra, suggesting substantial consumption of the vinyl groups during radical copolymerization.. No additional bands associated with side reactions were detected, that consistent with the formation of polymeric materials containing VPPI-derived emissive units.

STA was used to investigate the thermal stability and degradation behaviour of the monomers and their copolymers under a nitrogen atmosphere. The TGA curves of the copolymers are compared in Fig. 3a, while Fig. 3b shows a representative STA analysis of copolymer P(Th-VPPI-*co*-VK). The key thermal parameters are summarized in Table 1, and the complete STA curves, along with experimental details, are provided in the *ESI*.

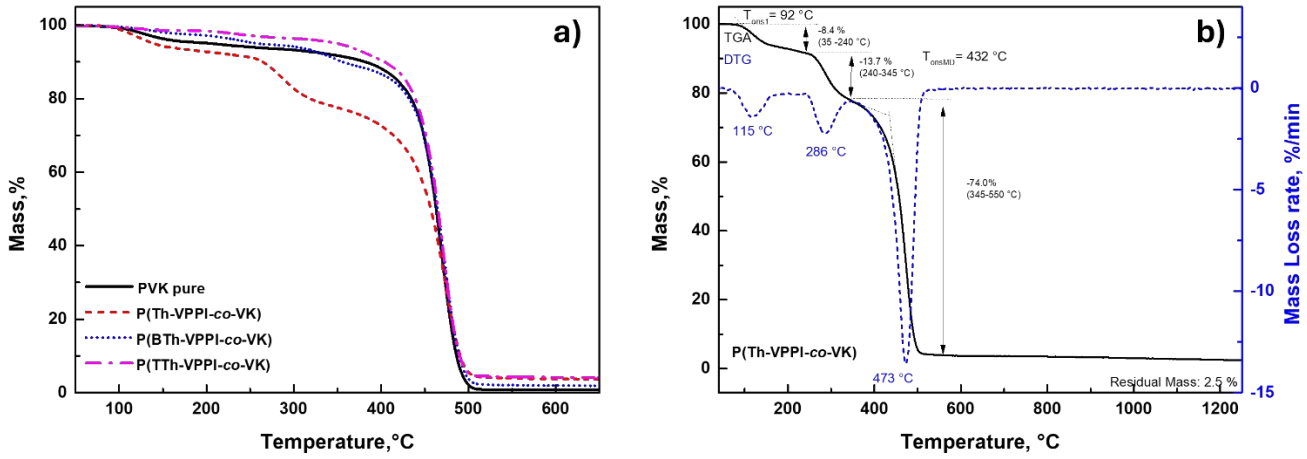

Figure 3. a) Thermogravimetric analysis (TGA) curves of synthesized copolymers recorded under nitrogen atmosphere; the temperature range is limited to 650 °C for clarity, as no further mass changes occur at higher temperatures; b) STA analysis of copolymer P(Th-VPPI-*co*-VK) demonstrating TGA (black) and DTG (blue, first derivative of TGA) curves with evaluation of the initial mass loss (T_{ons1}), onset of the main degradation step (T_{onsMD}), DTG maximum (T_{max}), mass-loss intervals, and residual mass.

Table 1. Thermal properties of phenanthroimidazole-based monomers and their copolymers were determined by STA (TGA/DTG/DSC) under a nitrogen atmosphere. T_5 and T_{10} denote temperatures at 5 % and 10 % mass loss, respectively. T_{onsMD} corresponds to the onset of the main degradation step. Residual mass values were evaluated at 600 °C and 1250 °C under a nitrogen atmosphere. T_{max} corresponds to the temperature of maximum weight loss rate, while T_m denotes the melting temperature.

	TGA					DTG	DSC
Name	**T_5, °C**	**T_{10}, °C**	**T_{onsMD}, °C**	**Residue at 600 °C, %**	**Residue at 1250 °C, %**	**T_{max}, °C**	**T_m, °C**
Th-VPPI	416	436	420	38.3	33.1	471	242
BTh-VPPI	442	462	443	37.5	32.3	502	279
TTh-VPPI	438	459	427	74.8	64.5	466	281
PVK pure	206	382	436	0.9	0.6	470	-
P(Th-VPPI-*co*-VK)	140	264	432	3.7	2.5	473	-
P(BTh-VPPI-*co*-VK)	259	356	435	2.0	1.3	471	-
P(TTh-VPPI-*co*-VK)	351	404	438	4.2	3.2	471	-

The copolymers exhibit an earlier onset of initial mass loss than the monomers, reflected by lower T_5 and T_{10} values, while the temperature of the main degradation step (T_{onsMD}) remains nearly unchanged. This behaviour is typical of polymeric materials and is commonly attributed to early degradation of side groups or structural rearrangements .[23] This initial mass loss is limited to some extent and does not involve significant degradation of the main polymer backbone. Importantly, the onset of the main degradation step (T_{onsMD}) remains nearly identical for monomers (420-443 °C) and copolymers (432-438 °C), indicating that the presence of VPPI-derived emissive units does not significantly alter the intrinsic thermal robustness of the chromophore-containing structure, despite noticeable differences in polymer molecular weight and dispersity among the copolymers. . These values are comparable to those reported for thermally stable phenanthroimidazole-based and

related luminescent polymer systems,[24] suggesting that polymer integration does not compromise the intrinsic thermal robustness of the chromophore.

Differences in degradation kinetics are further reflected in the temperature interval between T_5 and T_{10}. The monomers exhibit a narrow interval of approximately 20 °C, indicating a sharp onset of degradation, whereas the copolymers display much broader intervals of 53-176 °C, reflecting a more gradual, multistep initial mass loss. At elevated temperatures, monomers retain substantial residual mass due to pronounced char formation, while copolymers undergo nearly complete mass loss and show no further changes above 600 °C. The small residual mass observed for the copolymers (1.3–4.2 wt.% at 1250 °C) is broadly consistent with the low chromophore loading in the copolymer composition (5 wt.%) and the dominant volatilization of the PVK matrix during thermal degradation. Overall, the thermal analysis indicates that polymer integration primarily alters the degradation pathway and kinetics, while preserving the intrinsic thermal robustness of the emissive phenanthroimidazole core. The thermal stability of the prepared systems is comparable with other emissive organic materials reported in the literature. Phenanthroimidazole-based emitters typically exhibit decomposition temperatures around 400-430 °C, reflecting the high intrinsic thermal robustness of the aromatic chromophore core.[1,25] Similarly, carbazole-based emissive materials commonly used in optoelectronic applications show 5 % weight-loss temperatures in the range of approximately 350-480 °C.[26] In this context, the values obtained for the present systems (T5 = 416-442 °C for the monomers and T_{onsMD} ≈ 432-438 °C for the copolymers) fall well within the typical stability range reported for conjugated emissive polymer systems.

The molecular weight characteristics of the obtained copolymers were determined by size exclusion chromatography (SEC) equipped with multi-angle light scattering (MALS), refractive index (RI), and online viscometry detectors.[27,28] The measurements were performed in THF as the eluent, and the detailed experimental conditions are provided in the *ESI*. The obtained molecular weight parameters are summarized in Table 2. The synthesized copolymers exhibit number-average molar masses (M_n) ranging from 4,900 to 30,600 g/mol and weight-average molar masses (M_w) between 25,700 and 116,000 g/mol. Among the materials investigated, the highest molar mass averages were observed for the P(TTh-VPPI-*co*-VK) copolymer (M_n = 30,600 g/mol, M_w = 116,000 g/mol), indicating compatibility of the corresponding monomer with the applied radical polymerization conditions. In contrast, the P(Th-VPPI-*co*-VK) copolymer exhibited significantly lower molar masses (M_n = 4,900 g/mol, M_w = 25,700 g/mol), suggesting a lower degree of chain propagation under identical polymerization conditions.

The dispersity values (Đ = 3.8-5.3) indicate relatively broad molecular weight distributions, which can be attributed to the nature of free-radical copolymerization and the specific characteristics of the system. The intrinsic viscosity values determined by the online viscometer are generally consistent with the molar mass data. Notably, P(TTh-VPPI-*co*-VK) exhibits an intrinsic viscosity comparable to that of pure PVK despite its higher M_w, suggesting differences in polymer chain conformation or compactness in solution. The molecular parameters and intrinsic viscosity of this copolymer approach those of pure PVK, suggesting that the thieno[3,2-*b*]thiophene-containing monomer does not significantly hinder radical polymerization and allows efficient chain growth. Overall, the SEC results support the formation of polymeric materials under the applied radical copolymerization conditions and demonstrate that the nature of the heteroaromatic substituent influences the resulting molar mass distribution.

DFT quantum chemical calculations

To gain deeper insight into the electronic structure of the synthesized monomers, density functional theory (DFT) calculations were performed. All calculations were carried out using the Gaussian 16 software package[29] employing the B3LYP[30,31] functional with the 6-311+G(d,p) basis set together with the GD3BJ[32] empirical dispersion correction. Solvent effects corresponding to chloroform were included using the CPCM continuum solvation model.[33,34] The optimized molecular geometries together with selected frontier molecular orbitals (HOMO-1, HOMO, LUMO and LUMO+1) and the corresponding orbital energies are presented in Figure 4.

The optimized geometries reveal that the phenanthroimidazole core remains largely planar, while the attached aromatic substituents adopt slightly twisted conformations relative to the central conjugated scaffold.

Table 2. Molecular characteristics: the number-average molar mass (Mn), the weight-average molar mass (M_w), the z-average molar mass (M_z), the dispersity (M_w/M_n, Đ), and the weight-average intrinsic viscosity ($[\eta]_w$) of the prepared polyvinyl carbazole copolymers.

Name	M_n, g/mol	M_w, g/mol	M_z, g/mol	Đ	$[\eta]_w$, ml/g
PVK pure	18,700	84,600	225,000	4.5	19.4
P(Th-VPPI-*co*-VK)	4900	25,700	70,000	5.3	8.3
P(BTh-VPPI-*co*-VK)	13,800	57,300	113,000	4.2	13.7
P(TTh-VPPI-*co*-VK)	30,600	116,000	228,000	3.8	19.3

This moderate torsion is typical for phenanthroimidazole derivatives and helps to reduce excessive intermolecular π-π stacking while maintaining effective electronic communication within the conjugated system. Analysis of the frontier molecular orbitals shows a clear spatial distribution of electron density within the molecules. In all three compounds, the HOMO is mainly localized on the phenanthroimidazole core and partially extends toward the adjacent phenyl fragment. In contrast, the LUMO is predominantly distributed over the heteroaromatic substituent containing the thiophene, benzo[*b*]thiophene, or thieno[3,2-*b*]thiophene unit. Such an orbital distribution suggests that the lowest electronic transition has a partial intramolecular charge-transfer (ICT) character from the phenanthroimidazole framework toward the heteroaromatic fragment.

The calculated HOMO energy levels are very similar for all three monomers, ranging from -5.63 to -5.51 eV, while the

View Article Online
DOI: 10.1039/D6MA00406C

LUMO energies remain close to -1.9 eV. As a result, the calculated HOMO-LUMO energy gaps are also nearly identical (3.60-3.70 eV). These results indicate that variation of the heteroaromatic substituent from thiophene to benzo[*b*]thiophene or thieno[3,2-*b*]thiophene has only a limited influence on the overall electronic structure of the conjugated system.

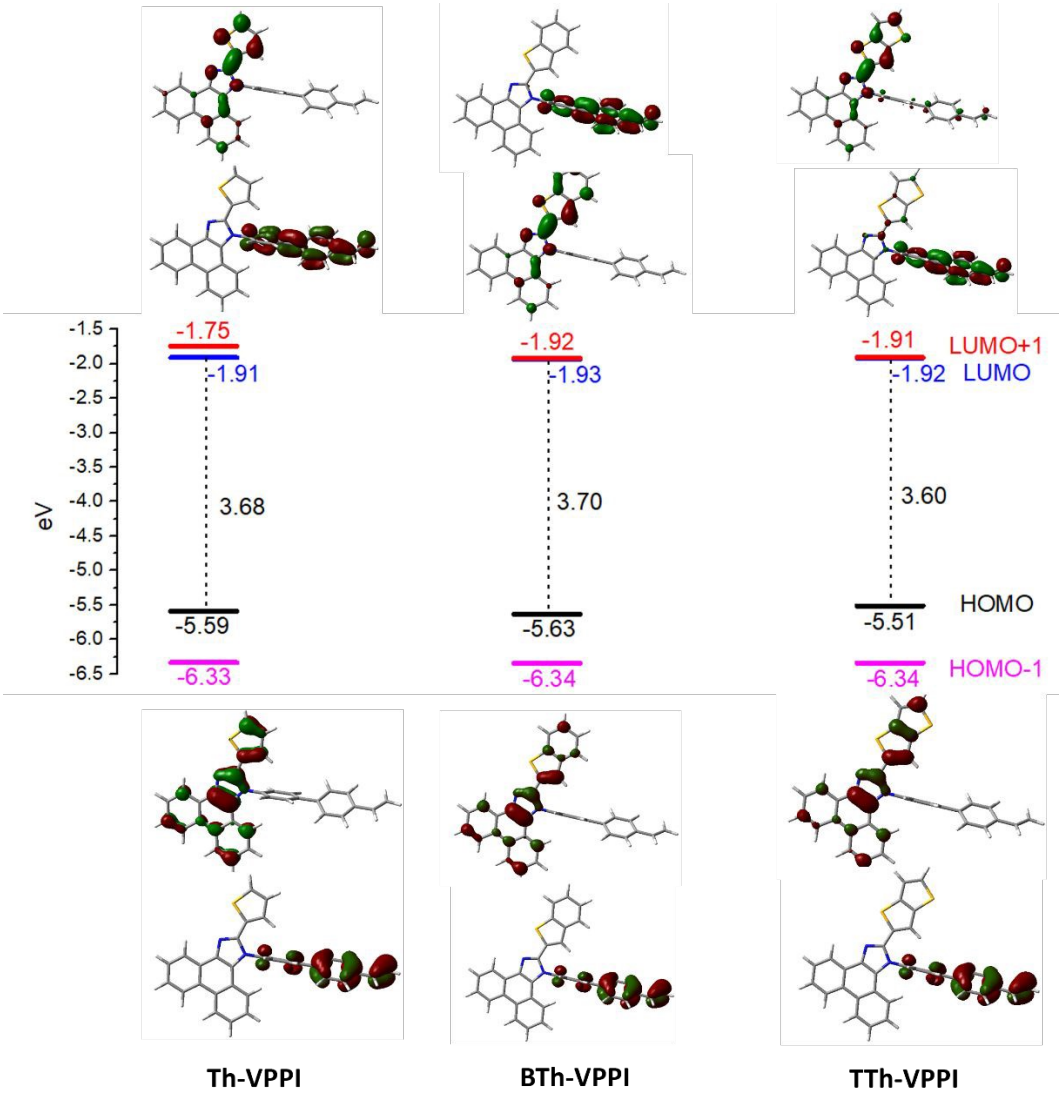

Figure 4. Energy level diagrams of monomers Th-VPPI, BTh-VPPI and TTh-VPPI.

A notable feature is the relatively small energy separation between the LUMO and LUMO+1 orbitals, particularly in the benzo[*b*]thiophene and thieno[3,2-*b*]thiophene derivatives. The presence of nearby unoccupied orbitals suggests several energetically accessible excited states, which may contribute to the photophysical behaviour's sensitivity to the surrounding environment. This observation is consistent with the experimentally observed emission behaviour of the compounds, both in solution and in polymer matrices. Inspection of the orbital shapes shows that HOMO-1 remains largely localized on the phenanthroimidazole core, while LUMO+1 is primarily associated with the heteroaromatic substituent. Although the benzo[*b*]thiophene derivative exhibits a slightly different spatial distribution of the frontier orbitals due to the increased rigidity and extended aromatic character of the fused ring system, the overall energy pattern across the series remains very similar. Overall, the theoretical results are in good agreement with the experimentally observed optical properties of the compounds and reproduce the general trends detected for the series.

To further elucidate the nature of the electronic transitions, time-dependent DFT (TD-DFT) calculations were performed for the optimized geometries. The lowest-energy absorption bands in all studied compounds were assigned predominantly to HOMO → LUMO transitions, consistent with the frontier orbital distributions discussed above (Fig.S42a). The calculated excitation energies (λ_{calc} ≈ 381-391 nm) are in good agreement

View Article Online
DOI: 10.1039/D6MA00486C

with the experimental absorption maxima, confirming the validity of the theoretical model (Table S3).

The corresponding oscillator strengths are significant for BTh-VPPI and TTh-VPPI (f ≈ 0.8-1.0), indicating allowed π-π* transitions within the conjugated system. In contrast, a lower oscillator strength was obtained for Th-VPPI, reflecting its less extended conjugation. Importantly, the analysis of the involved molecular orbitals shows that the electronic transitions are primarily localized within the phenanthroimidazole - thiophene framework, with negligible contribution from the N1 styryl fragment. This observation further supports the proposed electronic decoupling of the polymerizable moiety from the emissive core.

Electrochemical properties of the monomers were investigated by cyclic voltammetry (CV). The HOMO energy levels were estimated from the oxidation onset potentials, while the LUMO levels were calculated using the optical band gap values. The obtained values are in good agreement with the DFT results and optical measurements, supporting the proposed electronic structure (Table S2, Figure S42b).

Optical properties

Solution photophysics

The optical properties of the synthesized thiophene-engineered phenanthroimidazoles were first investigated in dilute solutions to assess the intrinsic photophysical behaviour of the molecular chromophores, free from intermolecular interactions. Normalized absorption, excitation, and emission spectra of the halogenated precursors and the corresponding vinyl-functionalized monomers are presented in Figure 5, while the key photophysical parameters are summarized in Table 3.

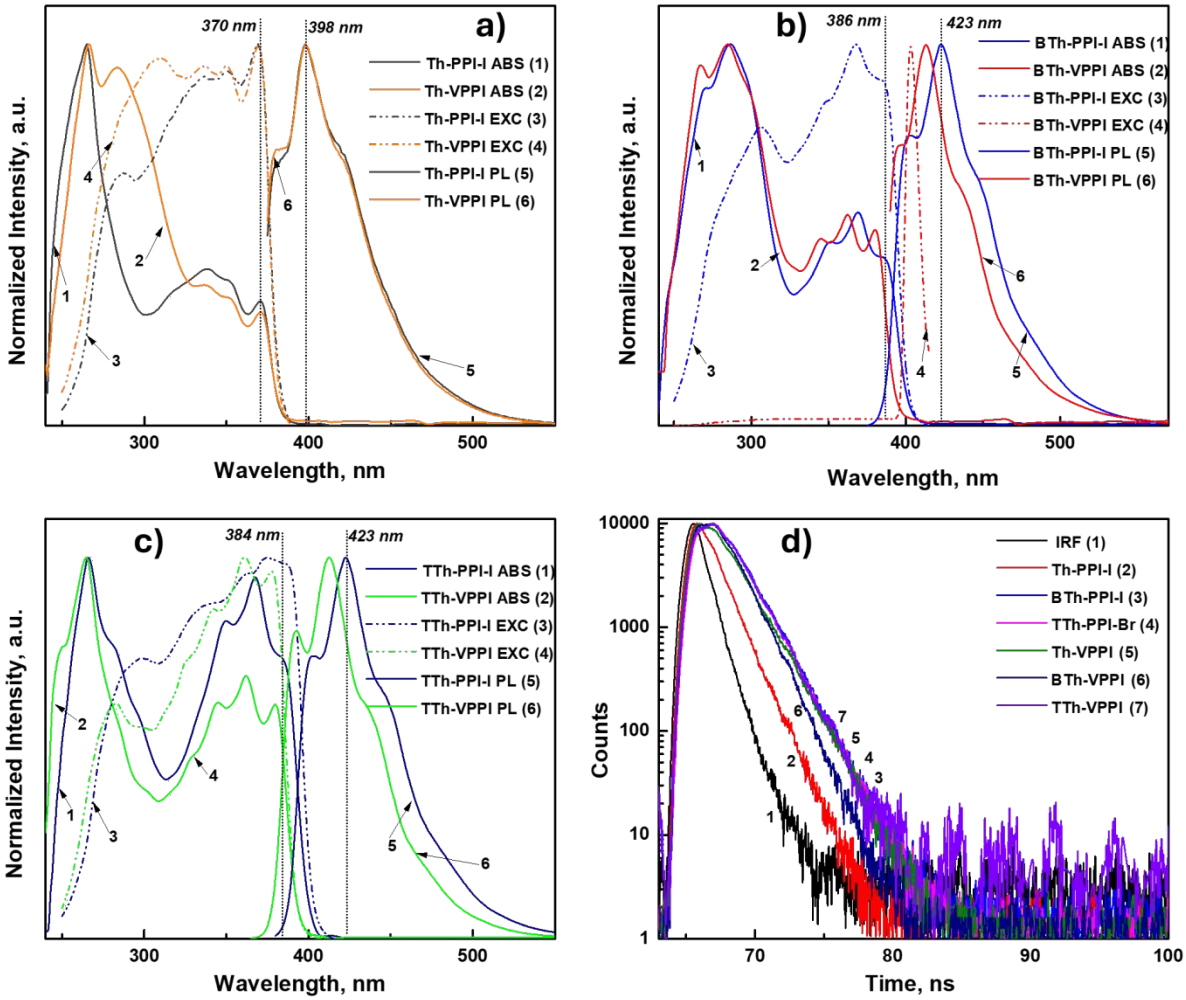

Figure 5. Normalized absorbance, excitation, and emission spectra of series monomers a) Th-VPPI; b) BTh-VPPI and c) TTh-VPPI; d)Time-resolved PL decay profiles of all synthesized compounds in $CHCl_3$ (λ_{exc} = 375 nm).

View Article Online
DOI: 10.1039/D6MA00406G

ARTICLE

Table 3. The key optical properties of the synthesized compounds.

Compound	λ_{ABS}, *nm*	λ_{EXC}, *nm*	λ_{PL}, *nm*	*Stokes shift, nm*	E_g, *eV*	τ_{avr}, *ns*	*PL QY, %*
Th-PPI-I	370	369	398	28	3.18	1.52	9.0
Th-VPPI	370	369	398	28	3.18	3.05	59.3
BTh-PPI-I	386	367	423	37	3.02	3.04	10.2
BTh-VPPI	380	403	413	33	3.08	2.46	70.7
TTh-PPI-Br	384	375	423	39	3.04	3.02	59.1
TTh-VPPI	379	360	412	33	3.09	2.74	86.4
PVK	343	344	404	61	3.42	16.45	2.7
P(Th-VPPI-co-VK)	386	383	419	33	3.09	2.17	20.2
P(BTh-VPPI-co-VK)	376	346	402	26	3.20	2.70	23.5
P(TTh-VPPI-co-VK)	394	335	430	36	3.03	1.91	23.2

All compounds exhibit structured absorption bands in the near-UV region (≈370-390 nm), which are characteristic of the rigid phenanthroimidazole π-conjugated core. The absorption profiles are largely preserved across the series, indicating that substitution at the C2 position with sulfur-containing heteroaromatic fragments does not dramatically perturb the ground-state electronic structure. Nevertheless, the position of the absorption onset shows a clear dependence on the nature of the thiophene-derived substituent, with BTh- and TTh-containing derivatives exhibiting a generally red-shifted onset compared to the Th analogues.[35] This trend reflects enhanced π-delocalization and a modest reduction of the optical band gap, in agreement with the calculated E_g values (Table 3).

The excitation spectra closely match the corresponding absorption profiles when monitored at the emission maxima, confirming that the observed emission arises from the same electronic transitions and that no additional emissive species form in solution. Upon excitation, all compounds display well-resolved blue-to-blue-green photoluminescence with a pronounced vibronic structure typical of phenanthroimidazole-based luminogens.[36]

The emission maxima are systematically shifted to longer wavelengths with increasing π-extension of the C2 substituent: Th derivatives emit around 398 nm, while BTh and TTh analogues exhibit emission in the 412-423 nm range. This bathochromic shift is accompanied by an increase in the Stokes shift, indicating greater excited-state relaxation in the more extended and rigid sulfur-containing systems.[37] Comparison between the halogenated precursors (Th-PPI-I, BTh-PPI-I, TTh-PPI-Br) and their vinyl-functionalized counterparts (Th-VPPI, BTh-VPPI, TTh-VPPI) reveals that introduction of the styryl moiety at the N1-aryl position has only a minor influence on the absorption and emission maxima. Thus, the differences in λ_{abs}, λ_{PL} and E_g between halogenated precursors and vinyl-functionalized derivatives are minimal (within a few nm and ~0.01-0.05 eV), providing quantitative evidence that the N1 styryl group is electronically decoupled from the emissive core. These all observations confirm that the vinyl group does not significantly extend the conjugation of the phenanthroimidazole core but instead acts as a chemically orthogonal functional handle. Interestingly, vinyl functionalization leads to a pronounced increase in PL QY compared to the corresponding halogenated precursors. This effect may originate from the removal of the heavy-atom effect associated with iodine or bromine substituents, which are known to enhance non-radiative decay through spin-orbit coupling. Importantly, the preservation of the spectral positions upon vinyl functionalization is essential for subsequent polymer integration, as it ensures that the intrinsic emissive properties of the chromophore are retained.

Time-resolved photoluminescence measurements further support this conclusion. The average excited-state lifetimes (τ_{avg}) of the vinyl-functionalized monomers are comparable to, or slightly shorter than, those of the corresponding halogenated precursors. This behaviour can be attributed to subtle changes in non-radiative decay pathways introduced by the styryl substituent, rather than to fundamental alterations of the excited-state electronic structure. Overall, the lifetime values in the nanosecond range are consistent with prompt fluorescence from locally excited states, with no indication of delayed emission or triplet harvesting processes under the investigated conditions.[35] Taken together, the solution-state photophysical data demonstrate that C2 thiophene-based substitution provides an effective handle to fine-tune the emission wavelength and optical gap of phenanthroimidazole chromophores, while N1 styryl functionalization preserves their intrinsic emissive characteristics. This combination of spectral tunability and chemical orthogonality represents a key advantage of the present molecular design.

Polymeric and film emission

To evaluate the behaviour of the thiophene-engineered phenanthroimidazoles in the solid state, the photophysical

properties of the synthesized copolymers P(Th-VPPI-*co*-VK), P(BTh-VPPI-*co*-VK), and P(TTh-VPPI-*co*-VK) were investigated in thin films. Incorporation of the emissive VPPI monomers into a poly(N-vinylcarbazole) (PVK) matrix provides a rigid, optically transparent host environment while reducing chromophore aggregation and phase separation, thereby enabling direct assessment of structure-property relationships in polymer-bound form.[38] PVK was selected as a model host polymer due to its good film-forming ability, optical transparency in the relevant spectral region, and its well-known role as a hole-transporting material in optoelectronic systems. A relatively low chromophore loading (5 wt.%) was intentionally selected to facilitate radical copolymerization while minimizing possible aggregation effects during polymerization and film formation.

The absorption spectra of the copolymer films (Figure 6a) exhibit broad bands in the near-UV region, dominated by the PVK matrix, with superimposed contributions from the phenanthroimidazole chromophores. Compared to neat PVK, the copolymer films display a clear bathochromic (P(Th-VPPI-*co*-VK) and P(TTh-VPPI-*co*-VK)) and hypsochromic (P(BTh-VPPI-*co*-VK)) shift of the absorption edge, reflecting the presence of the thiophene-substituted phenanthroimidazole units. Notably, the relative positions of the absorption onsets follow the same trend observed in solution, indicating that the electronic structure of the VPPI chromophores is largely preserved after radical copolymerization.[39]

Upon photoexcitation, all copolymer films exhibit intense blue to blue-green emission (Figure 6b), with spectral profiles that remain structured but are slightly broadened compared to those in dilute solution. The emission maxima are systematically shifted relative to the corresponding monomers, which can be attributed to a combination of the dielectric constant of the polymer environment and restricted conformational relaxation in the solid state. As in solution, the emission wavelength of the copolymer films depends sensitively on the nature of the C2 sulfur-containing substituent. While the TTh-based copolymer exhibits the most red-shifted emission, the BTh derivative shows a comparatively blue-shifted response, highlighting that conjugation topology and rigidity, rather than formal π-extension alone, govern the solid-state emission behaviour. Among the three systems, P(TTh-VPPI-*co*-VK) exhibits the most red-shifted emission (≈430 nm), consistent with the highest degree of conjugation and sulfur content.[40] Notably, the TTh-VPPI derivative exhibits a remarkably high photoluminescence quantum yield (86%), which is significantly higher than that typically reported for phenanthroimidazole-based luminogens.

Time-resolved photoluminescence measurements of the copolymer films (Figure 6c) reveal mono- to weakly multiexponential decay profiles with average lifetimes in the range of 1.9-2.7 ns (Table 3). These values are significantly shorter than those of pristine PVK (τ_{avg} ≈ 16.5 ns), confirming that the emission of the copolymer films originates predominantly from the phenanthroimidazole chromophores rather than from the host matrix.[41] The relatively narrow distribution of lifetime values across the series suggests a relatively uniform emissive response across the investigated polymeric materials and the absence of strong excimer or aggregate emission. Importantly, no additional low-energy emission bands or long-lived components were detected in the copolymer films, suggesting reduced aggregation-induced quenching relative to physically blended systems and interchromophoric interactions. This behaviour contrasts with physically doped systems, where phase separation and concentration-dependent quenching often complicate the interpretation of solid-state emission. The results indicate that the characteristic emissive behavior of the VPPI chromophores is retained in the polymeric materials.. Importantly, the copolymers retain efficient photoluminescence despite the incorporation of the chromophores into the polymer backbone.[17] Within the studied range, variations in molecular weight and dispersity do not lead to systematic changes in optical properties, confirming that the emission behavior is dominated by the chromophore structure rather than polymer chain parameters.

Overall, the polymer-bound photophysical properties closely mirror the trends observed in solution, indicating that the thiophene-based C2 substitution remains the dominant factor governing the emissive behaviour, while the N1 styryl group enables preliminary evaluation of the emissive monomers in polymeric materials without major perturbation of their optical behavior. These findings highlight the suitability of thiophene-engineered VPPI monomers for the preparation of emissive polymeric materials retaining substituent-dependent photophysical trends.

Structure-property correlations

The present series enables a direct assessment of how the nature of the C2 sulfur-containing substituent influences the photophysical properties of phenanthro[9,10-*d*]imidazoles in both molecular and polymer-bound forms. Although thiophene (Th), benzo[*b*]thiophene (BTh), and thieno[3,2-*b*]thiophene (TTh) represent a progression in structural rigidity and annellation.

View Article Online
DOI: 10.1039/D6MA00406G

ARTICLE

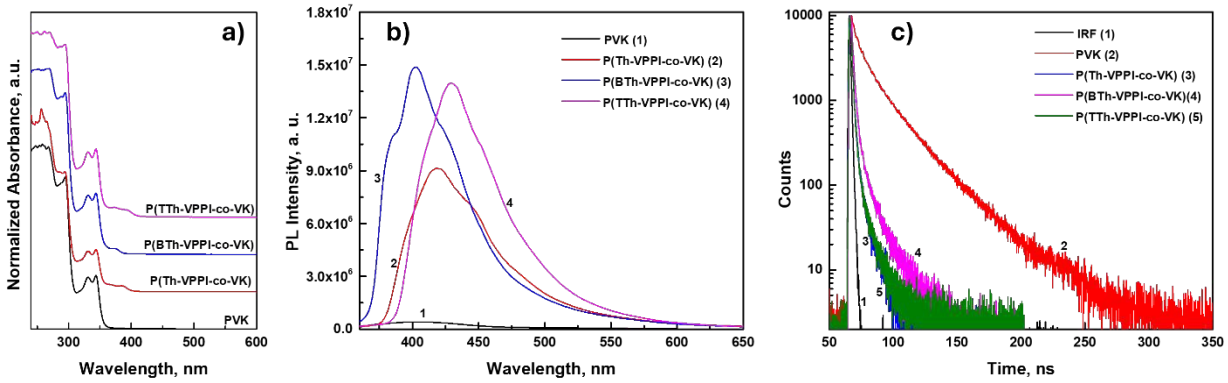

Figure 6. Absorbance (a), emission (b) and PL decay kinetic curves (c) of synthesized copolymers in thin films.

The resulting optical trends are non-monotonic, indicating that conjugation topology and electronic coupling play a more important role than formal π-extension alone. Such deviations from a simple π-extension trend likely arise from subtle differences in torsional angles and electronic coupling between the heteroaromatic fragment and the phenanthroimidazole core.

In solution, substitution at the C2 position leads to noticeable differences in absorption and emission characteristics. While all derivatives exhibit absorption maxima in a relatively narrow spectral window, the emission response is more sensitive to the nature of the sulfur-containing fragment. Th-based compounds show the most blue-shifted emission, whereas BTh and TTh derivatives display red-shifted photoluminescence. Notably, the BTh-substituted systems emit at longer wavelengths than Th analogues but do not exceed the red shift observed for the TTh derivatives, which exhibit the lowest optical band gaps and the most bathochromically shifted emission. This behaviour suggests that increased annellation and heteroatom density enhance excited-state delocalization, but the extent of electronic communication between the C2 substituent and the phenanthroimidazole core depends sensitively on molecular geometry. The Stokes shifts follow a similar non-linear trend. BTh- and TTh-containing compounds generally display larger Stokes shifts than their Th analogues, indicating a greater degree of excited-state relaxation. This effect is consistent with increased structural rigidity and altered vibrational coupling in the fused sulfur-containing systems, rather than a simple increase in conjugation length.

Introduction of the styryl group at the N1-aryl position has only a marginal influence on the photophysical parameters in solution. The absorption and emission maxima, as well as the optical band gaps, remain largely unchanged upon vinyl functionalization, confirming that the N1 styryl moiety is electronically decoupled from the emissive phenanthroimidazole core.[16]

Upon incorporation into the poly(N-vinylcarbazole) backbone, the same structure-property relationships are largely preserved in thin films. The copolymer emission maxima do not follow a monotonic Th < BTh < TTh sequence. Instead, the BTh-based copolymer exhibits a comparatively blue-shifted emission relative to the Th analogue, whereas the TTh-containing copolymer shows the most red-shifted photoluminescence. This observation highlights that solid-state emission is governed not only by intrinsic chromophore structure but also by subtle differences in chromophore-polymer interactions and conformational constraints imposed by the polymer matrix. Time-resolved photoluminescence measurements further support these correlations. All VPPI-based copolymers display nanosecond-scale excited-state lifetimes that are significantly shorter than those of pristine PVK, suggesting predominant localization of excitation on the phenanthroimidazole units. Variations in lifetime across the series are modest and do not correlate directly with emission wavelength, indicating that radiative and non-radiative decay pathways are influenced by local environment and molecular rigidity rather than by optical band gap alone. Overall, the data demonstrate that C2 sulfur-containing substitution provides a powerful but non-trivial means of tuning the optical properties of phenanthroimidazoles.[17] Rather than following a simple π-extension trend, the photophysical behaviour reflects a balance between conjugation topology, structural rigidity, and chromophore-environment interactions. This nuanced structure-property relationship is preserved upon polymer integration, underscoring the robustness of the molecular

View Article Online
DOI: 10.1039/D6MA00406G

design and its suitability for the development of luminescent polymeric materials.

Conclusions

A series of thiophene-engineered phenanthro[9,10-*d*]imidazoles combining C2 sulfur-containing aromatic substitution with N1 styryl functionality has been designed and synthesized, providing a modular platform for correlating molecular structure with photophysical behaviour in both molecular and polymer-bound forms. Thiophene, benzo[*b*]thiophene, and thieno[3,2-*b*]thiophene fragments were systematically introduced at the C2 position to probe the influence of conjugation topology and rigidity, while the N1 styryl group served as a polymerizable handle without extending the emissive π-system. Photophysical investigations demonstrate that C2 sulfur-based substitution enables effective tuning of emission properties; however, the observed trends are non-monotonic and governed by the interplay between conjugation topology, structural rigidity, and electronic coupling to the phenanthroimidazole core rather than by formal π-extension alone. Vinyl functionalization at the N1 position has only a minor impact on the intrinsic optical characteristics, confirming its electronic isolation from the emissive core.

The incorporation of the vinyl-functionalized chromophores into a poly(N-vinylcarbazole) backbone yields luminescent materials whose solid-state emission reflects the same substituent-dependent behaviour observed in solutions. The absence of aggregation-induced quenching and long-lived emissive components highlights the advantage of chemical attachment over physical blending. This work establishes a rational design strategy in which electronic tuning and processability are decoupled within a single phenanthroimidazole scaffold, offering a robust foundation for the development of luminescent polymers with tunable optical behaviour suitable for further development of luminescent polymeric materials.

Author contributions

L. Loghina: writing - original draft, methodology, investigation, formal analysis, data curation, and conceptualization. J. Jancalek, Z. Zmrhalova, R. Jambor, Z. Ruzickova, A. Imramovsky, S. Podzimek and M. Vlcek: formal analysis, data curation, visualization, and writing - review and editing. R. Jambor, M. Vlcek: supervision and project administration.

Conflicts of interest

There are no conflicts to declare.

Data availability

All supporting data are included in the article and its *ESI*. Detailed experimental sections, NMR spectroscopy, FTIR spectroscopy, additional TGA data, DFT calculation, crystallography data and characterization.

Data for the crystal structure reported in this article have been deposited at the Cambridge Crystallographic Data Centre (CCDC) under the deposition numbers 2528847-2528849.

The datasets generated during and/or analysed during the current study are available in the Figshare repository, DOI: 10.6084/m9.figshare.31645174.

Acknowledgements

This work has been funded by a grant from the Programme Johannes Amos Comenius under the Ministry of Education, Youth and Sports of the Czech Republic [No. CZ.02.01.01/00/23_021/0008593], and by a grant LM2023037 from the Ministry of Education, Youth and Sports of the Czech Republic.

References

1 J. Tagare and S. Vaidyanathan, Recent development of phenanthroimidazole-based fluorophores for blue organic light-emitting diodes (OLEDs): an overview, *J. Mater. Chem. C*, 2018, **6**, 10138. https://doi.org/10.1039/C8TC03689F
2 M. Idris, C. Coburn, T. Fleetham, J. Milam-Guerrero, P. I. Djurovich, S. R. Forrest and M. E. Thompson, Phenanthro[9,10-d]triazole and imidazole derivatives: high triplet energy host materials for blue phosphorescent organic light emitting devices, *Mater. Horiz.*, 2019, **6**, 1179. https://doi.org/10.1039/C9MH00195F
3 E. Dhineshkumar, N. Arumugam, E. Manikandan, M. Maaza and A. Mandal, Fabrication of high performance based deep-blue OLED with benzodioxin-6-amine-styryl-triphenylamine and carbazole hosts as electroluminescent materials, *Sci. Rep.*, 2024, **14**, 2432. https://doi.org/10.1038/s41598-023-50867-x
4 Y. Wang, C. Du, Z. Cheng, S. Ge, Z. Feng, L. Wan, Y. Hu, X. Ma, Z. Su and P. Lu, Rational Molecular Design of Phenanthroimidazole-Based Fluorescent Materials toward High-Efficiency Deep-Blue OLEDs by Molecular Isomer Engineering, *ACS Appl. Mater. Interfaces*, 2024, **16**, 38, 51201. https://doi.org/10.1021/acsami.4c05510
5 J. Jayabharathi, S. Panimozhi and V. Thanikachalam, Asymmetrically twisted phenanthrimidazole derivatives as host materials for blue fluorescent, green and red phosphorescent OLEDs, *Sci. Rep.*, 2019, **9**, 17555. https://doi.org/10.1038/s41598-019-54125-x
6 H. Debus, Ueber die Einwirkung des Ammoniaks auf Glyoxal, *Justus Liebigs Ann. Chem.*, 1858, **107**, 199. https://doi.org/10.1002/jlac.18581070209
7 S. Saxer, C. Marestin, R. Mercier and J. Dupuy, The multicomponent Debus–Radziszewski reaction in macromolecular chemistry, *Polym. Chem.*, 2018, **9**, 1927. https://doi.org/10.1039/C8PY00173A
8 C.-J. Kuo, T.-Y. Li, C.-C. Lien, C.-H. Liu, F.-I. Wu and M.-J. Huang, Bis(phenanthroimidazolyl)biphenyl derivatives as saturated blue emitters for electroluminescent devices, *J. Mater. Chem.*, 2009, **19**, 1865. https://doi.org/10.1039/B816327H
9 V. Thanikachalam, E. Sarojpurani, J. Jayabharathi and P. Jeeva, Efficient phenanthroimidazole-styryl-triphenylamine derivatives for blue OLEDs: a combined experimental and theoretical study, *New J. Chem.*, 2017, **41**, 2443. https://doi.org/10.1039/C6NJ03801H

10 J. Huo, C. Gao, Y. Cao, H. Shi and B. Z. Tang, Rational design of phenanthroimidazole derivatives with hybridized local and charge-transfer characteristics to achieve efficient blue emission in non-doped OLEDs, *J. Mater. Chem. C*, 2023, **11**, 445. https://doi.org/10.1039/D2TC04957K

11 V. H. K. Fell, N. J. Findlay, B. Breig, C. Forbes, A. R. Inigo, J. Cameron, A. L. Kanibolotsky and P. J. Skabara, Effect of end group functionalisation of small molecules featuring the fluorene–thiophene–benzothiadiazole motif as emitters in solution-processed red and orange organic light-emitting diodes, *J. Mater. Chem. C*, 2019, **7**, 3934. https://doi.org/10.1039/C8TC02993H

12 A. Capan, H. Veisi, A. C. Goren and T. Ozturk, Concise Syntheses, Polymers, and Properties of 3-Arylthieno[3,2-*b*]thiophenes, *Macromolecules*, 2012, **45**, 20, 8228. https://doi.org/10.1021/ma301604e

13 S. M. K. A. Naqvi, F. Abbas, S. Bibi, M. K. Shehzad, N. Alhokbany, Y. Zhu, H. Long, R. B. Vasiliev, Z. and S. Chang, Theoretical investigation of benzodithiophene-based donor molecules in organic solar cells: from structural optimization to performance metrics, *RSC Adv.*, 2024, **14**, 29942. https://doi.org/10.1039/D4RA04818K

14 X. Wenta, L. Binbin, C. Xinyi, L. Mengke, Q. Zhenyang, T. Xiaohui, L. Kunkun, G. Cheng, M. Yuguang and S. Shi-Jian, Thiophene Disubstituted Benzothiadiazole Derivatives: An Effective Planarization Strategy Toward Deep-Red to Near-Infrared (NIR) Organic Light-Emitting Diodes, *Frontiers in Chemistry*, 2019, **7**, 276. https://doi.org/10.3389/fchem.2019.00276

15 S. Kula, A. Szlapa-Kula, M. Filapek, K. Bujak, S. Kotowicz, M. Siwy, J. Grzelak, M. Szalkowski, S. Maćkowski, E. Schab-Balcerzak, Novel phenanthro[9,10-d]imidazole derivatives - effect of thienyl and 3,4-(ethylenedioxy)thienyl substituents, *Synthetic Metals*, 2019, **251**, 40. https://doi.org/10.1016/j.synthmet.2019.03.022

16 A. Szlapa-Kula and S. Kula, Progress on Phenanthroimidazole Derivatives for Light-Emitting Electrochemical Cells: An Overview, *Energies*, 2023, **16**, 13, 5194. https://doi.org/10.3390/en16135194

17 L. Loghina, J. Machotova, R. Svoboda, J. Houdek, M. Kohl, Z. Ruzickova, R. Jambor and M. Vlcek, Photoluminescent phenanthroimidazole derivatives as covalently linked UV stabilizers for latex coatings, *RSC Adv.*, 2025, **15**, 28827. https://doi.org/10.1039/D5RA05109F

18 N. Noormofidi and C. Slugovc, Optical response of phenantroimidazole-dyes covalently linked to a polynorbornene-backbone to acid and base6 *Eur. Polym. J.*, 2010, **46**, 4, 694. https://doi.org/10.1016/j.eurpolymj.2010.01.006

19 J. Mei, N. L. C. Leung, R. T. K. Kwok, J. W. Y. Lam, B. Z. Tang, Aggregation-Induced Emission: Together We Shine, United We Soar!, *Chem. Rev.*, 2015, **115**, 21, 11718. https://doi.org/10.1021/acs.chemrev.5b00263

20 N. K. S. Teo, B. Fan, A. Ardana and S. H. Thang, Aggregation-induced emission polymers via reversible-deactivation radical polymerization, *Aggregate*, 2024, **5**, 1, 414. https://doi.org/10.1002/agt2.414

21 P. Pyykkö and M. Atsumi, Molecular Single-Bond Covalent Radii for Elements 1–118, *Chem. – Eur. J.*, 2009, **15**, 186. https://doi.org/10.1002/chem.200800987

22 C. E. Corcione and M. Frigione, Characterization of Nanocomposites by Thermal Analysis, *Materials*, 2012, **5**, 12, 2960. https://doi.org/10.3390/ma5122960

23 Y.-X. Wang, C.-N. Chuang, C.-L. Chang, Y.-T. Wu, C.-Y. Chang, M.-k. Leung, Post-functionalized poly(N-vinylcarbazole)s as effective low turn-on-voltage phosphorescent-hosts in polymeric light emitting devices, *European Polymer Journal*, 2014, **52,** 227. https://doi.org/10.1016/j.eurpolymj.2013.12.017

24 J.-x. Luo, C.-l. Yang, D.-w. Zhou, L.-y. Liang, M.-g. Lu, Novel polymeric light-emitting devices based on bipolar copolymers containing quinoline aluminum moieties and N-vinylcarbazole segments, *Synthetic Metals*, 2011, **161**, 15. https://doi.org/10.1016/j.synthmet.2011.05.029

25 Z.-L. Zhu, S.-F. Ni, W.-C. Chen, M. Chen, J.-J. Zhu, Y. Yuan, Q.-X. Tong, F.-L. Wong and C.-S. Lee, Tuning electrical properties of phenanthroimidazole derivatives to construct multifunctional deep-blue electroluminescent materials, *J. Mater. Chem. C*, 2018, **6**, 3584. https://doi.org/10.1039/c7tc04972b

26 R. Beresneviciute, A. Kumar, D. Blazevicius, S. Lenka, S.-T. Hsieh, M.-F. Tsai, G. Krucaite, D. Tavgeniene, J.-H. Jou, S. Grigalevicius, Carbazolyl Electron Donor and Pyridinyl Electron Acceptor Containing Derivatives as Potential Host Materials for Green Organic Light-Emitting Diodes, *Molecules*, 2025, **30**, 9, 1911. https://doi.org/10.3390/molecules30091911

27 P. J. Wyatt, Light scattering and the absolute characterization of macromolecules, *Anal. Chim. Acta*, 1993, **272**, 1, 1. https://doi.org/10.1016/0003-2670(93)80373-S

28 A. M. Striegel, Viscometric Detection in Size-Exclusion Chromatography: Principles and Select Applications, *Chromatographia*, 2016, **79**, 94. https://doi.org/10.1007/s10337-016-3078-0

29 M. J. Frisch, G. W. Trucks, H. B. Schlegel, *et al.*, Gaussian 16, Revision A.03, *Gaussian*, Inc., Wallingford, CT, 2016.

30 A. D. Becke, Density-functional thermochemistry. III. The role of exact exchange, *J. Chem. Phys.*, 1993, **98**, 5648. https://doi.org/10.1063/1.464913

31 C. Lee, W. Yang and R. G. Parr, Development of the Colle-Salvetti correlation-energy formula into a functional of the electron density, *Phys. Rev. B*, 1988, **37**, 785. https://doi.org/10.1103/PhysRevB.37.785

32 S. Grimme, S. Ehrlich and L. Goerigk, Effect of the damping function in dispersion corrected density functional theory, *J. Comput. Chem.*, 2011, **32**, 1456. https://doi.org/10.1002/jcc.21759

33 V. Barone and M. Cossi, Quantum Calculation of Molecular Energies and Energy Gradients in Solution by a Conductor Solvent Model, *J. Phys. Chem. A*, 1998, **102**, 11, 1995. https://doi.org/10.1021/jp9716997

34 M. Cossi, N. Rega, G. Scalmani and V. Barone, Energies, structures, and electronic properties of molecules in solution with the C-PCM solvation model, *J. Comput. Chem.*, 2003, **24**, 669. https://doi.org/10.1002/jcc.10189

35 S. Kula, A. Szlapa-Kula, S. Kotowicz, M. Filapek, K. Bujak, M. Siwy, H. Janeczek, S. Maćkowski and E. Schab-Balcerzak, Phenanthro[9,10-*d*]imidazole with thiophene rings toward OLEDs application, *Dyes Pigm.*, 2018, **159**, 646. https://doi.org/10.1016/j.dyepig.2018.07.014

36 Y. Zhang, S.-L. Lai, Q.-X. Tong, M.-Y. Chan, T.-W. Ng, Z.-C. Wen, G.-Q. Zhang, S.-T. Lee, H.-L. Kwonge and C.-S. Lee, Synthesis and characterization of phenanthroimidazole derivatives for applications in organic electroluminescent devices, *J. Mater. Chem.*, 2011, **21**, 8206. https://doi.org/10.1039/C1JM10326A

37 S. Gan, S. Hu, X.-L. Li, J. Zeng, D. Zhang, T. Huang, W. Luo, Z. Zhao, L. Duan, S.-J. Su and B. Z. Tang, Heavy Atom Effect of Bromine Significantly Enhances Exciton Utilization of Delayed Fluorescence Luminogens, *ACS Appl. Mater. Interfaces*, 2018, **10**, 20, 17327. https://doi.org/10.1021/acsami.8b05389

38 T. Ye, J. Chena and D. Ma, Electroluminescence of poly(N-vinylcarbazole) films: fluorescence, phosphorescence and electromers, *Phys. Chem. Chem. Phys.*, 2010, **12**, 15410. https://doi.org/10.1039/C0CP00461H

View Article Online
DOI: 10.1039/D6MA00406G

39 S. Y. Park, S. Choi, G. E. Park, H. J. Kim, C. Lee, J. S. Moon, S. W. Kim, S. Park, J. H. Kwon, M. J. Cho and D. H. Choi, Unconventional Three-Armed Luminogens Exhibiting Both Aggregation-Induced Emission and Thermally Activated Delayed Fluorescence Resulting in High-Performing Solution-Processed Organic Light-Emitting Diodes, *ACS Appl. Mater. Interfaces*, 2018, **10**, 17, 14966. https://doi.org/10.1021/acsami.7b19681

40 H. Xu, R. Zhu, P. Zhao, L.-H. Xie and W. Huang, Photophysical and electroluminescent properties of a Series of Monochromatic red-emitting europium-complexed nonconjugated copolymers based on diphenylphosphine oxide modified polyvinylcarbazole, *Polymer*, 2011, 52, **3**, 804. https://doi.org/10.1016/j.polymer.2010.12.016

41 D. C. Santos, G. de S. Barros, M. de F. V. Marques, Enhancing Blue Emission in Poly(N-vinylcarbazole): Synthesis, Functionalization with Anthracene, and Mitigation of Aggregation-Caused Quenching, *ACS Omega*, 2025, **10**, 34, 39250. https://doi.org/10.1021/acsomega.5c06357

View Article Online
DOI: 10.1039/D6MA00406G

Data Availability Statement

The datasets generated and analyzed during the current study - including FTIR, UV-Vis, PL, and TGA data - are available in the **Figshare** repository: **https://doi.org/10.6084/m9.figshare.31645174**

Synthesis methods, characterization methods, crystallography, DFT calculations, TGA data, ^{1}H, ^{13}C NMR, and FTIR spectra of the synthesized compounds are also provided in the Electronic Supplementary Information (ESI).

Data for the crystal structure reported in this article have been deposited at the Cambridge Crystallographic Data Centre (CCDC) under the deposition numbers 2528847-2528849.